

Green CdSe/CdSeS Core/Alloyed-Crown Nanoplatelets Achieve Unity Photoluminescence Quantum Yield over a Broad Emission Range

An Hu, Peng Bai, Yunke Zhu, Zeguo Song, Ruotao Wang, Jiangchang Zheng, Yige Yao, Qu Zhang, Zhengping Ding, Peng Gao, Xinyu Sui, Xinfeng Liu, and Yunan Gao*

Cadmium-based nanoplatelets as optical display and lasing materials are widely explored and exhibit great advantages, owing to their narrow emission linewidths, anisotropic transition-dipole distributions, and low lasing thresholds. However, in the green range, the photoluminescence quantum yield (PLQY) and emission tunability of nanoplatelets are still inferior to that of quantum dots. In this work, a new synthesis protocol is developed, enabling core/crown nanoplatelets to grow continuously from elementary precursors to their final form. A new heterostructure of CdSe/CdSeS core/alloyed-crown nanoplatelets is produced that realizes 100% PLQY, the continuous tunability of emission peaks in between 502 and 550 nm, and low full-width-at-half-maximum (FWHM) of less than 15 nm. Achieving these excellent properties in all three aspects at the same time is unprecedented. In addition, the time-resolved photoluminescence (TRPL) spectra of these nanoplatelets show a mono-exponential decay characteristic, and the nanoplatelet film can also show 100% PLQY and a mono-exponential decay characteristic, indicating the suppression of trap states. The high-quality nanoplatelets achieved in this work provide a solid foundation for developing nanoplatelet-based light sources, like light-emitting diodes and lasers, with much higher efficiency, color purity, and lower working thresholds.

1. Introduction

Excellent optical properties and solution processability have made colloidal semiconductor nanocrystals promising materials for photonic applications.^[1–3] Cadmium-based nanoplatelets, in particular, exhibit narrow emission linewidths, anisotropic transition-dipole distributions, giant modal gain coefficients, and ultra-low lasing thresholds.^[4–10] Compared to other colloidal emitters, like quantum dots, nanorods, and perovskites nanocrystals, cadmium-based nanoplatelets have narrower linewidths, higher color purity, and can thus fulfill the next-generation display criterion of the Rec. 2020 (refs. [11–15]). Owing to controllable dipole distributions, the external quantum efficiency (EQE) of nanoplatelet-based light-emitting diodes (NP-LEDs) can reach a theoretic limit of about 40%, which is 1.5 times the theoretic limit in quantum dot based LEDs.^[16] Besides, cadmium-based nanoplatelets are reported to demonstrate

A. Hu, P. Bai, Y. Zhu, Z. Song, R. Wang, J. Zheng, Y. Yao, Q. Zhang, Y. Gao

State Key Laboratory for Artificial Microstructure and Mesoscopic Physics
School of Physics
Peking University
Beijing 100871, P. R. China
E-mail: gyn@pku.edu.cn

Z. Ding, P. Gao
Electron Microscopy Laboratory
School of Physics
Peking University
Beijing 100871, P. R. China

X. Sui, X. Liu
CAS Key Laboratory of Standardization and Measurement for Nanotechnology
CAS Center for Excellence in Nanoscience
National Center for Nanoscience and Technology
Beijing 100190, P. R. China

X. Sui, X. Liu
University of Chinese Academy of Sciences
Beijing 100049, P. R. China

Y. Gao
Frontiers Science Center for Nano-optoelectronics
Beijing 100871, P. R. China

Y. Gao
Collaborative Innovation Center of Extreme Optics
Shanxi University
Taiyuan 030006, P. R. China

Y. Gao
Peking University Yangtze Delta Institute of Optoelectronics
Nantong, Jiangsu 226010, P. R. China

 The ORCID identification number(s) for the author(s) of this article can be found under <https://doi.org/10.1002/adom.202200469>.

DOI: 10.1002/adom.202200469

low lasing thresholds and continuous-wave lasing at room temperature.^[9,17]

However, the application of cadmium-based nanoplatelets (such as the high efficiency and color purity NP-LEDs, nanoplatelet lasing) requires the improvement of photoluminescence quantum yield (PLQY) and emission tunability. In the red range, near-unity PLQY nanoplatelets, 19% EQE NP-LEDs, and $0.8 \mu\text{J cm}^{-2}$ threshold lasing have been achieved.^[2,8,18] As for in the green range, the current highest PLQYs of nanoplatelets are 90%@515 nm (4.5 MLs, i.e., five Cd monolayers and four Se monolayers) and 60%@550 nm (5.5 MLs), leaving a room for the improvement of PLQYs (Table S1, Supporting Information).^[11,19–21] Moreover, exploration for high PLQY nanoplatelets in other green ranges is in demand. Despite several emission tuning methods such as elementary alloying,^[22–24] altering quantum confinement,^[25–28] and ligand engineering,^[29,30] high PLQYs and the broad tunable range of those synthesized nanoplatelets are not well guaranteed (Table S2, Supporting Information). PLQYs are affected by deep and shallow traps, which can be reflected in the time-resolved photoluminescence (TRPL) spectra.^[29–31] Deep trap states can decrease PLQY by a large percent and add a short channel to the TRPL. Shallow trap states can trap and de-trap excitons. Hence, shallow trap states can decrease PLQY by a small percent and add a long-lived tail to the TRPL. Currently, cadmium-based nanoplatelets including blue, green, and red emission nanoplatelets have not realized a well suppression to shallow trap states.^[18,20,32] Besides, the PLQY of nanoplatelets in the film, which is usually lower than PLQYs of nanoplatelets in dispersion, still needs improvement, since it can directly affect EQEs of NP-LEDs.^[11,18] The realization of high PLQYs, the mono-exponential decay, and the tunable green emission nanoplatelets in both dispersion and film has remained a tough challenge.

In this work, we report the synthesis of high-quality cadmium-based nanoplatelets in the green range, which have a unity PLQY and a mono-exponential decay characteristic in TRPL spectra. These nanoplatelets are composed of the CdSe core and the CdSeS gradually alloyed crown. With the controlled lateral confinement on the CdSe core and the growth of the CdSeS crown, we can tune the emission peak from 502 to 550 nm and achieve high PLQYs at the same time. In addition, these CdSe/CdSeS core/alloyed-crown nanoplatelets exhibit excellent optical and chemical stabilities. Smooth films with high PLQY and mono-exponential decay characteristic in TRPL spectra can be fabricated, showing great potentials in realizing high-EQEs NP-LEDs. Overall, the results lay a solid foundation for the utilization of cadmium-based nanoplatelets as excellent optical materials.

2. Results and Discussion

We develop a new synthesis protocol, where the core/crown nanoplatelets can grow continuously from elementary precursors to their final form. The seamless growth not only simplifies the synthesis operation but also substantially improves the optical properties of PLQY and emission tunability. **Figure 1a** illustrates the protocol. The addition of cadmium acetate dihydrate ($\text{Cd}(\text{Ac})_2$), which triggers the lateral growth of

CdSe nanoplatelets,^[33] is recorded here as time “0 min.” After a certain period of CdSe growth, we add a sulfur precursor into the same reaction flask via a syringe pump. A sulfur introduction case for the CdSe/CdSeS nanoplatelets with the final emission peak at 550 nm is shown in **Figure 1b**, where sulfur is injected at a linear rate lasting from the 5th to the 10th min, forming the final structure illustrated in **Figure 1a**. Small volumes are sampled during the synthesis and PLQYs are measured. **Figure 1b** shows a linear correlation between sulfur injection and PLQY increase (from $\approx 20\%$ to 95%).

Accompanying the increase of PLQY, the long-lived tail in TRPL caused by shallow traps are suppressed by the crown growth, as shown in **Figure S1** (Supporting Information). These shallow traps can be further suppressed by degassing at 110 °C at the end of the synthesis to remove H_2S that is a reaction intermediate and can lead to trap states (**Figure S2**, Supporting Information).^[34] Finally, $\approx 100\%$ PLQY and the mono-exponential decay characteristic are obtained, as shown in **Figure 1d**. This characteristic indicates the suppression of both deep and shallow trap states, so excitons decay almost solely via intrinsic radiative recombination.

The heterostructure of these nanoplatelets is characterized as CdSe/CdSeS core/gradually alloyed-crown. In the absorption spectra shown in **Figure 1c**, a notable increase, centered at 450 nm covering a broad region, can be seen from the samples taken at the 6th, 8th, and 10th min. This broad absorption increase suggests the formation of a CdSeS alloyed crown, because it does fall into the CdS absorption region but doesn't have the sharp peak of a pure CdS crown observed in CdSe/CdS core/crown nanoplatelets.^[19,20] The energy-dispersive X-ray spectroscopy (EDS) scanning tunneling electron microscope (STEM) image of a single edge-up nanoplatelet with emission at 550 nm is shown in **Figure 1e**, which reveals that the crown is gradually alloyed. The Cd is evenly distributed throughout the nanoplatelet while Se and S show complementary distributions without a clear boundary. The gradual alloying is consistent with the synthesis protocol, where the sulfur concentration is gradually increased during the crown formation phase (Phase 2 in **Figure 1a**). There are weak signals of S in the CdSe core area which may result from the projection of a three-dimensional structure onto a two-dimensional TEM image.

Apart from PLQY, the new protocol pilots nanoplatelets toward much better emission tunability, another critical property of optical materials. In 5.5 MLs CdSe nanoplatelet synthesis, one can see a clear red-shift of the emission peak from ≈ 525 to ≈ 550 nm occurring in a few minutes (**Figure 2a,b** black trace). This is caused by a series of effects: at first, vertical growth is rapid, CdSe seeds soon reach the designed thickness at the end of the 1st min; then, lateral growth is perceived, with relaxation of lateral quantum confinement, which is reflected in the observed red-shift lasting for the 1st–10th min.^[33,35,36] This observation suggests that the emission peak can be continuously tuned from 525 to 550 nm in 5.5 MLs CdSe nanoplatelets, if the lateral growth can be precisely tuned. This approach is feasible under our new synthesis protocol.

We find that the red-shift, corresponding to the lateral growth of the CdSe core, can be inhibited by adding the S precursor. Since the CdSe core has a lower bandgap than the CdSeS crown, its size is decisive to the emission peak position.

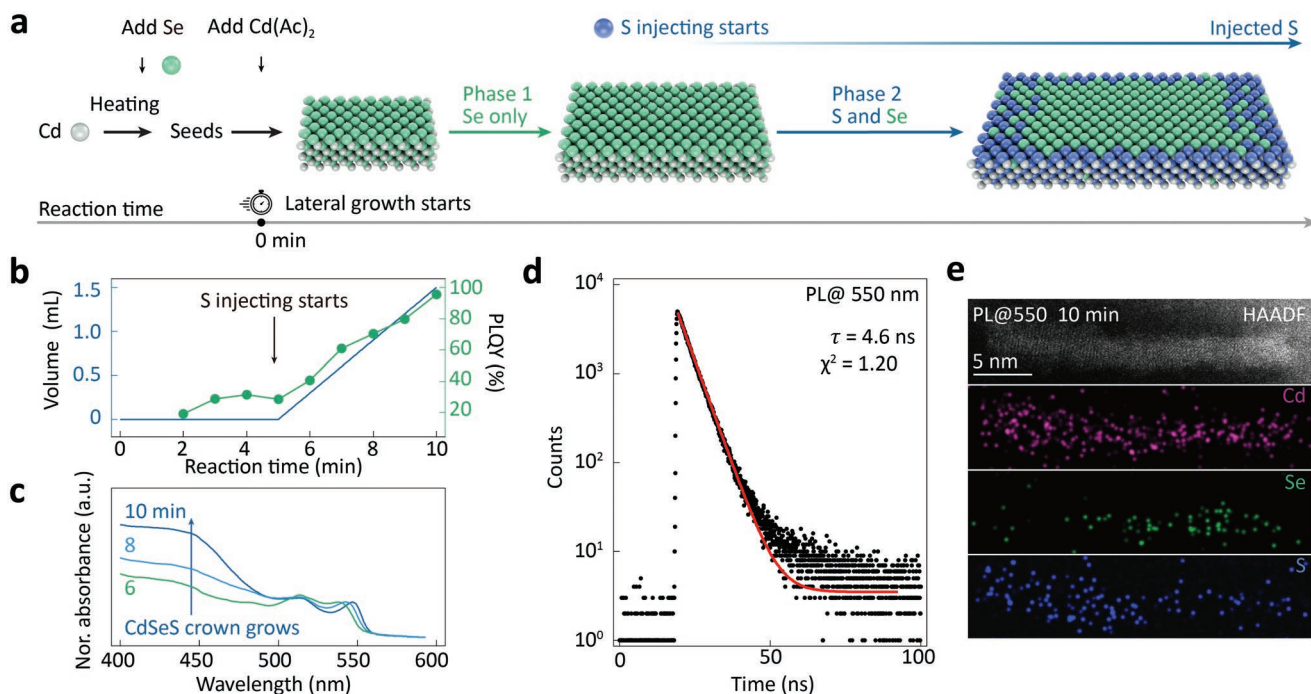


Figure 1. a) The schematic representation of the synthesis for 5.5 monolayers (MLs) CdSe/CdSeS core/alloyed-crown nanoplatelets with the emission peak at 550 nm. Gray, green, and blue balls represent Cd, Se, and S, respectively. The top Cd layer is hidden for the clarity of vision. b) Left-axis and the blue line denote the volume of injected sulfur precursor during the synthesis of 550 nm nanoplatelets. Right-axis and the green dots denote the PLQYs. Addition of Cd(Ac)₂ is defined as “0 min.” c) Absorption spectra of 550 nm nanoplatelets extracted at 6th, 8th, and 10th min. d) The time-resolved photoluminescence of 550 nm nanoplatelets. Black dots are raw data, and the red line is a mono-exponential decay fitting. e) High-angle annular dark-field scanning transmission electron microscope (HAADF-STEM) and EDS-STEM elemental mapping images of edge-up 550 nm core/alloyed-crown nanoplatelets extracted at 10th min.

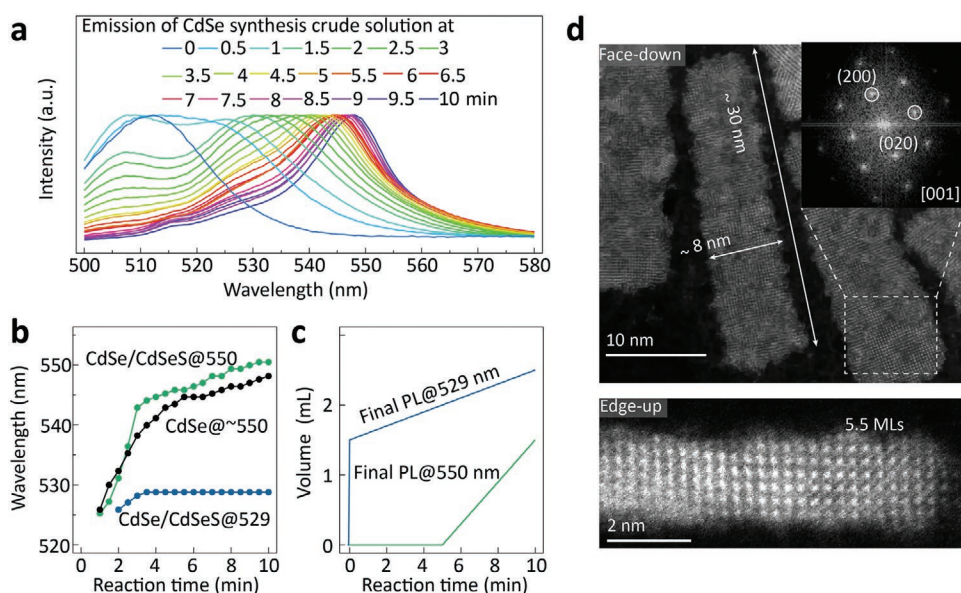


Figure 2. a) Emission evolution of crude solution during the synthesis of 5.5 MLs CdSe nanoplatelets from 0 to 10 min, showing a distinct red-shift. b) Evolution of emission peak during the synthesis of CdSe nanoplatelets with a final peak at 549 nm (black trace), CdSe/CdSeS core/crown nanoplatelets with a final peak at 550 nm (green trace), and CdSe/CdSeS core/crown nanoplatelets with a final peak at 529 nm (blue trace). c) Sulfur precursor injection curves of two the kinds of CdSe/CdSeS core/crown nanoplatelets. d) HAADF-STEM images of CdSe/CdSeS nanoplatelets with an emission peak at 545 nm in face-down and edge-up configurations. Inset in panel (d): diffraction patterns measured along the [001] axis.

Hence, by changing the injection condition of the S precursor, the emission peak can be precisely tuned. Figure 2b gives the emission peak evolution of two kinds of representative CdSe/CdSeS core/crown nanoplatelets. With a delayed sulfur injection at 5th min, the CdSe/CdSeS core/crown nanoplatelets with a final emission peak at 550 nm are synthesized. The red-shift of these nanoplatelets (green trace) and of pure CdSe nanoplatelets (black trace) are shown. In comparison, with an early and quick injection of S, the red-shift (blue trace) stops at 529 nm. Note that the above-mentioned CdSe/CdSeS nanoplatelets have similar lengths and widths (Figure S3, Supporting Information), suggesting that the different emission positions stem from different core sizes.

The HAADF-STEM is used to reveal the crystal structure of these CdSe/CdSeS core/alloyed-crown nanoplatelets. Nanoplatelets with an emission peak at 545 nm are used. Figure 2d shows high-resolution images of several nanoplatelets. The diffraction pattern in the inset of Figure 2d reveals a zincblende crystal structure. An atom-resolved STEM image from an edge-up nanoplatelet, Figure 2d lower panel, shows exactly how many atomic layers are present. In these 545 nm emission nanoplatelets, there are six layers of Cd atoms and five layers of Se and/or S atoms along the normal direction forming 5.5 MLs, with a total thickness of ≈ 1.6 nm. The atomic layer numbers and the thickness are the same as pure CdSe with an emission peak at 550 nm, suggesting our method would not alter the thickness of nanoplatelets.^[37] Additional TEM images

and absorbance of nanoplatelets are presented in Figures S3 and S4 (Supporting Information).

Figure 3a shows the results from continuously tuning the emission positions from 525 to 550 nm for 5.5 MLs nanoplatelets, from 502 to 515 nm for 4.5 MLs nanoplatelets, with the FWHMs all below 15 nm (minimum of 8 nm). They all have unity PLQY and mono-exponential decay characteristics, as shown in Figure 3b, underlying that the exact intrinsic exciton lifetime can be determined without any disturbance of trap states. In nanoplatelets with the same thickness, the intrinsic exciton lifetimes of nanoplatelets increase as the lateral confinement increase. Lifetimes increase from 3.8 to 5.5 ns as emission shift from 512 to 502 nm for 4.5 MLs nanoplatelets and from 4.6 to 9.7 ns as emission shift from 550 to 529 nm for 5.5 MLs nanoplatelets (Figures 1d and 3b). The difference in excitation lifetime could be interpreted by the different oscillator strength caused by different extent of overlap between electron and hole wavefunctions. As the lateral confinement strengthens, i.e., the core size gets smaller, the electron wave function spreads more into the crown while the hole wave function still stays inside the core since CdS have a weak confinement on electrons in CdSe.^[38] For clarity, only representative peaks are shown in Figure 3, and additional data is included in Table S1 (Supporting Information). As a result of narrow FWHMs, locations of nanoplatelets emissions on the CIE color chromaticity diagram are close to the boundary (Figure 3c), indicating high color purity. The CdSe/CdSeS core/alloyed-crown nanoplatelets,

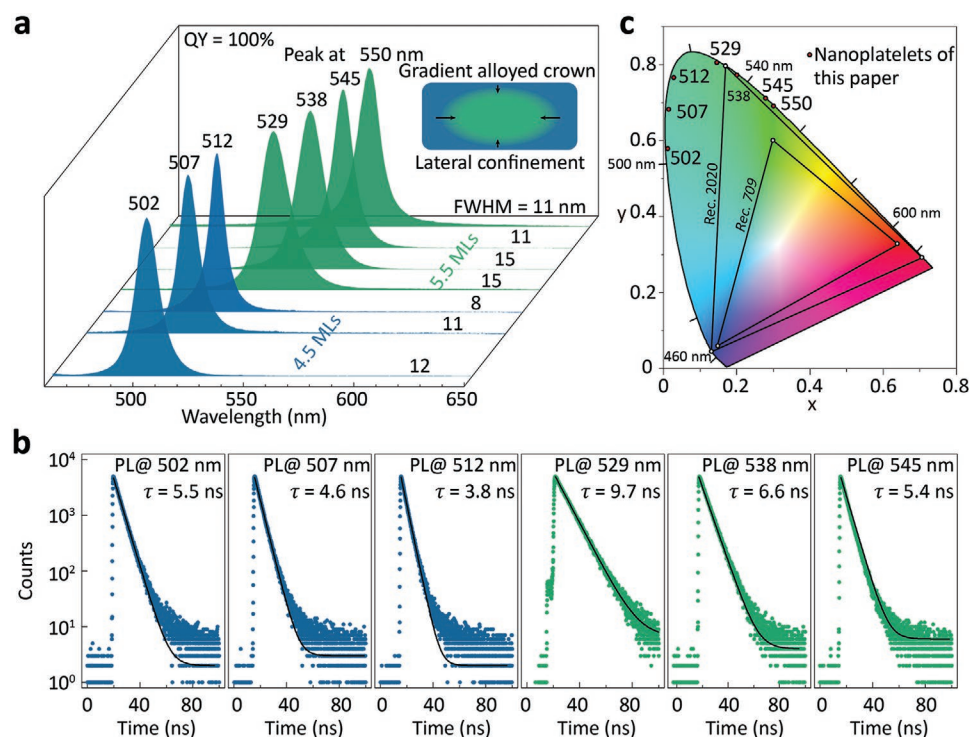


Figure 3. a) Steady emission spectra of a series of CdSe/CdSeS core/alloyed-crown nanoplatelets. 5.5 MLs nanoplatelets consist of 6 layers of Cd atoms and 5 layers of Se and/or S atoms. The range of 502–515 nm tuning is achieved on 4.5 MLs nanoplatelets (in blue), and on 5.5 MLs nanoplatelets for the remaining range (in green). b) Time-resolved photoluminescence of the nanoplatelets with emission peaks at 502, 507, 512, 529, 538, and 545 nm. Black lines are single exponential decay fitting. c) Locations of the emission of CdSe/CdSeS nanoplatelets (red dots) on International Commission on Illumination (CIE) chromaticity diagram.

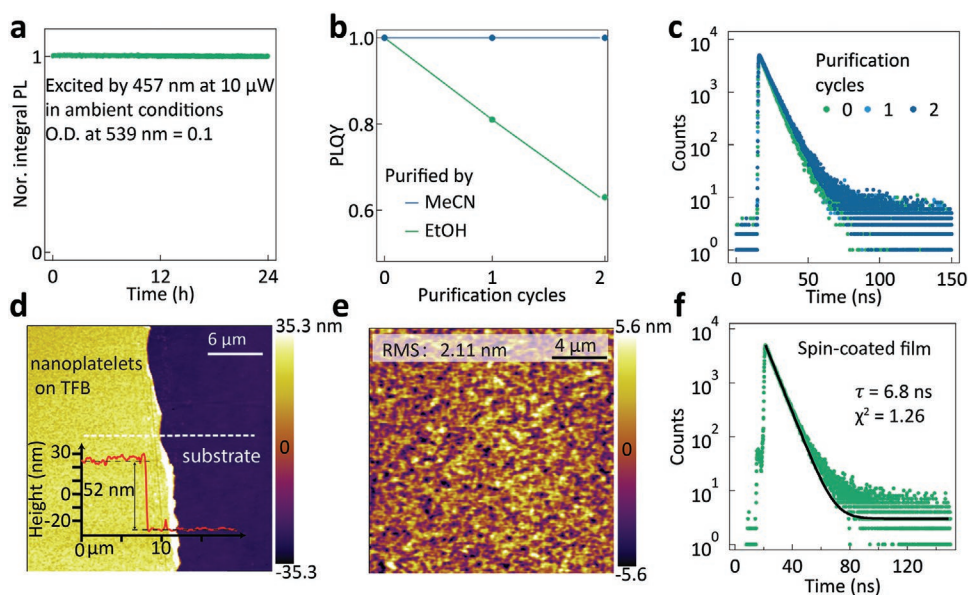


Figure 4. a) A normalized integral PL trace of nanoplatelets showing no change under 24 h optical excitation. b) The effect of purification cycles and anti-solvent on PLQYs of nanoplatelets. c) TRPL spectra of nanoplatelets after purifications using acetonitrile. d) An AFM image of spin-coated nanoplatelets film on the hole transport-layer TFB (39 nm thick). e) The root mean square (RMS) of the nanoplatelet film. f) Time-resolved photoluminescence of the CdSe/CdSeS core/crown nanoplatelet film with an emission peak at 529 nm.

with an emission at 529 and 15 nm FWHM, can cover the Rec 2020 color gamut with a coverage factor of 102% (Figure 3c).

Besides, these nanoplatelets possess high chemical and optical stabilities. Figure 4a presents a trace of continuous photoluminescence measurements 24 h under ambient conditions without stirring. There is no observable decay, great colloidal (no precipitation or aggregation) and optical (no bleaching) stabilities. The PLQY remains unchanged after two months storage under ambient conditions, implying a good stability. To test the chemical stability, we purify nanoplatelets using acetonitrile (MeCN) and ethanol (EtOH). After two cycles of purification using MeCN, the PLQY and single exponential decay feature of the nanoplatelets (centered at 538 nm) remain unchanged, as shown in Figure 4b,c. However, when using ethanol as an anti-solvent, the PLQY decreases after purification. The results are consistent with previous studies that MeCN is a ligand-friendly anti-solvent while EtOH can strip ligands.^[39,40]

From these high-quality CdSe/CdSeS core/alloyed-crown nanoplatelets, smooth films having high PLQYs can be fabricated. Figure 4d presents an atomic force microscopy (AFM) image of these nanoplatelets spin-coated on Poly[(9,9-dioctylfluorenyl-2,7-diyl)-co-(4,4'-(N-(4-sec-butylphenyl) diphenylamine))] (TFB), a widely used hole transport material in nanocrystal-based LEDs. The film thickness is 52 nm, and the TFB layer is 39 nm. The root mean square (RMS) is 2.11 nm, which is the same smoothness level of nanocrystal-based LEDs with high EQEs.^[1,18] Encouragingly, the spin-coated nanoplatelet film shows the mono-exponential decay characteristic, as shown in Figure 4f, indicating the suppression of trap-states. PLQYs and TRPLs of 545, 538, and 529 nanoplatelets in drop-casted films are also measured, and their χ^2 for the mono-exponential decay fitting of TRPLs are estimated (Figure S5, Supporting

Information). The increase of the long-lived tail, which could be caused by the reabsorption in nanoplatelets or the shallow trap states, will come with the increase of χ^2 . Their χ^2 in dispersion (1.16, 1.00, and 0.93, respectively) have lower values than in films (2.97, 1.54, and 1.18, respectively), implying the reabsorption effect or the shallow trap states is enhanced in condensed films. Their first exciton absorbance peak decreases as emission blue-shift, causing the decrease of reabsorption, as shown in Figures S4 and S6 (Supporting Information). Hence, the long-lived tail is best suppressed in 529 nanoplatelets. These nanoplatelets in dispersion all have 100% PLQYs, whereas in films shows lower or equal PLQYs (91%, 95%, and 100%, respectively), suggesting the film PLQY can also be improved with alleviated reabsorption which can avoid the photons absorbance by few non-perfect nanoplatelets.

3. Conclusion

To conclude, we realize high-performance CdSe/CdSeS core/alloyed-crown nanoplatelets with 100% PLQYs and mono-exponential decay characteristics covering a broad emission range (502–550 nm) by a new synthesis protocol. Smooth thin films with high PLQY and mono-exponential decay characteristics can be also produced using spin-coating, a method commonly used to fabricate nanocrystal-based LEDs. These exceptional optical properties ensure that these nanoplatelets have great potential in developing highly efficient NP-LEDs with supreme color-gamut coverage. Overall, the CdSe/CdSeS core/alloyed-crown nanoplatelets presented in this work exhibit exceptional optical properties, and thus lay a solid foundation for a broad range of photonic applications and also for fundamental studies.

4. Experimental Section

Chemicals: Chemicals were used directly without any purification: Selenium powder (Se, 200 mesh, Sigma-Aldrich 99.999%), sulfur (Sigma-Aldrich 99.98% trace metals basis), 1-octadecene (ODE, Sigma-Aldrich 95%), cadmium acetate dihydrate ($\text{Cd}(\text{Ac})_2 \cdot 2\text{H}_2\text{O}$, Sigma-Aldrich 98%), oleic acid (OAc, Sigma-Aldrich 90%), sodium myristate (TCI 98%), cadmium nitrate tetrahydrate (Sigma-Aldrich 99%), hexane (Honeywell HPLC), methanol (Fisher HPLC), ethanol (EtOH, Fisher HPLC), chloroform (Tongguang AR), acetonitrile (Sigma-Aldrich HPLC). Poly[(9,9-dioctylfluorenyl-2,7-diyl)-co-(4,4'-(N-(4-sec-butylphenyl)diphenylamine)] (TFB, American Dye Source, average molecular weight, $\approx 50\,000\text{ g mol}^{-1}$).

Precursor Preparation: Cadmium myristate was synthesized following a previous work.^[35] Briefly, cadmium nitrate tetrahydrate (1.23 g) was dissolved in methanol (40 mL), and sodium myristate (3.13 g) was dissolved in methanol (250 mL). Two chemicals were fully dissolved with the help of sonication for 15 min, and the two solutions were mixed and stirred for 2 min. The resulting white precipitate of $\text{Cd}(\text{myristate})_2$ was filtered and was rinsed 5 times with fresh methanol. Finally, the $\text{Cd}(\text{myristate})_2$ was dried under vacuum overnight.

Se suspension (Se-Sus) was prepared by dispersing Se powder (79 mg, 1 mmol) in ODE (10 mL) by sonication for 10 min. S suspension (S-Sus) was prepared by dispersing sulfur powder (32 mg, 1 mmol) in ODE (10 mL) by sonication for 30 min. S suspension with OAc (S-Sus-OAc) was prepared by mixing S-Sus (6 mL) with OAc (200 μL).

Synthesis of 550 nm Core/Alloyed-Crown Nanoplatelets: Here, a typical synthesis is presented, more synthesis details are included in the Supporting Information. For nanoplatelets with an emission peak at 550 nm, cadmium myristate (170 mg) in ODE (15 mL) was degassed under vacuum at room temperature for 10 min in a three-necked flask. Then the mixture was heated up to 250 °C rapidly under nitrogen. At 250 °C, 0.1 M Se (1.5 mL) suspended in ODE was injected. After 60 s, cadmium acetate dihydrate (80 mg) was rapidly added. After 5 min, S-Sus-OAc (1.5 mL) began to inject at 18 mL h^{-1} . After the injection was completed, the mixture was cooled down to 110 °C by air. OAc (0.3 mL) was injected at 160 °C during the cooling process. The whole mixture was degassed for 15 min at 110 °C to remove H_2S and then cooled to room temperature for purification.

Purification of Nanoplatelets: The crude reaction solution was mixed with EtOH (5 mL) and centrifuged for 10 min at 4000 rpm. The supernatant was discarded. The precipitate was dispersed in hexane (10 mL). The solution was mixed with MeCN (5 mL) and chloroform (5 mL) and centrifuged for 10 min at 10 000 rpm, and the supernatant was discarded. Finally, the precipitate was dispersed in hexane (20 mL) and stored.

Preparation of the Nanoplatelet Film on TFB: The TFB solution (in chlorobenzene, 8 mg mL^{-1}) was spin-coated onto the glass substrate at 2000 rpm for 45 s and backed at 150 °C for 30 min. Then the nanoplatelet solution (in octane, $\approx 4\text{ mg mL}^{-1}$) was spin-coated onto the substrate at 2000 rpm for 45 s.

Characterization: The time-resolved photoluminescence was measured by a time-correlated single-photon counting (TCSPC) spectrofluorometer (FLS1000, Edinburgh Instrument) with a 450 nm picosecond pulsed laser at a repetition frequency of 2 MHz. The peak count of all measurements was 5000, and the number of channels was 8192. The PL lifetime τ and the χ^2 was obtained by fitting the TRPL by a mono-exponential decay. The absolute PLQYs of samples on a spectrum calibrated system (FLS1000, Edinburgh) including Xe-lamp, integrating sphere, and visible photomultiplier tube were measured. The samples were in cuvettes with stirring. The HAADF-STEM and EDS-STEM measurements were conducted on an aberration-corrected FEI Titan Themis G2 microscope with an accelerating voltage of 300 kV. The EDS-STEM mapping was acquired on a Bruker Super-X EDS four-detector with a beam current of $\approx 50\text{ pA}$ and counts ranging from 1k cps to 2k cps for $\approx 10\text{ min}$. The TEM measurements were conducted on FEI Tecnai T20 with an accelerating voltage of 200 kV.

Supporting Information

Supporting Information is available from the Wiley Online Library or from the author.

Acknowledgements

This work was supported by the National Key R&D Program of China (Grant No. 2018YFA0306302), the National Natural Science Foundation of China (Grant No. 61875002), and Beijing Natural Science Foundation (Grant No. Z190005).

Conflict of Interest

The authors declare no conflict of interest.

Data Availability Statement

The data that support the findings of this study are available from the corresponding author upon reasonable request.

Keywords

nanoplatelets, core/alloyed-crown structure, green-color emission, mono-exponential decay, unity photoluminescence quantum yield

Received: February 28, 2022

Revised: March 20, 2022

Published online: April 15, 2022

- [1] X. Dai, Z. Zhang, Y. Jin, Y. Niu, H. Cao, X. Liang, L. Chen, J. Wang, X. Peng, *Nature* **2014**, *515*, 96.
- [2] Y. S. Park, J. Roh, B. T. Diroll, R. D. Schaller, V. I. Klimov, *Nat. Rev. Mater.* **2021**, *6*, 382.
- [3] T. Kim, K.-H. Kim, S. Kim, S.-M. Choi, H. Jang, H.-K. Seo, H. Lee, D.-Y. Chung, E. Jang, *Nature* **2020**, *586*, 385.
- [4] S. Ithurria, B. Dubertret, *J. Am. Chem. Soc.* **2008**, *130*, 16504.
- [5] S. Ithurria, M. D. Tessier, B. Mahler, R. P. S. M. Lobo, B. Dubertret, A. L. Efros, *Nat. Mater.* **2011**, *10*, 936.
- [6] Y. Gao, M. C. Weidman, W. A. Tisdale, *Nano Lett.* **2017**, *17*, 3837.
- [7] M. Li, M. Zhi, H. Zhu, W.-Y. Wu, Q.-H. Xu, M. H. Jhon, Y. Chan, *Nat. Commun.* **2015**, *6*, 8513.
- [8] N. Taghipour, S. Delikanli, S. Shendre, M. Sak, M. Li, F. Isik, I. Tanriover, B. Guzelurk, T. C. Sum, H. V. Demir, *Nat. Commun.* **2020**, *11*, 3305.
- [9] J. Q. Grim, S. Christodoulou, F. Di Stasio, R. Krahne, R. Cingolani, L. Manna, I. Moreels, *Nat. Nanotechnol.* **2014**, *9*, 891.
- [10] P. Bai, A. Hu, Y. Liu, Y. Jin, Y. Gao, *J. Phys. Chem. Lett.* **2020**, *11*, 4524.
- [11] F. Zhang, S. Wang, L. Wang, Q. Lin, H. Shen, W. Cao, C. Yang, H. Wang, L. Yu, Z. Du, J. Xue, L. S. Li, *Nanoscale* **2016**, *8*, 12182.
- [12] L. Protesescu, S. Yakunin, M. I. Bodnarchuk, F. Krieg, R. Caputo, C. H. Hendon, R. X. Yang, A. Walsh, M. V. Kovalenko, *Nano Lett.* **2015**, *15*, 3692.
- [13] H. Cao, J. Ma, L. Huang, H. Qin, R. Meng, Y. Li, X. Peng, *J. Am. Chem. Soc.* **2016**, *138*, 15727.
- [14] W. K. Bae, J. Kwak, J. W. Park, K. Char, C. Lee, S. Lee, *Adv. Mater.* **2009**, *21*, 1690.

- [15] H. Shen, Q. Gao, Y. Zhang, Y. Lin, Q. Lin, Z. Li, L. Chen, Z. Zeng, X. Li, Y. Jia, S. Wang, Z. Du, L. S. Li, Z. Zhang, *Nat. Photonics* **2019**, *13*, 192.
- [16] W. D. Kim, D. Kim, D.-E. Yoon, H. Lee, J. Lim, W. K. Bae, D. C. Lee, *Chem. Mater.* **2019**, *31*, 3066.
- [17] Z. Yang, M. Pelton, I. Fedin, D. V. Talapin, E. Waks, *Nat. Commun.* **2017**, *8*, 143.
- [18] B. Liu, Y. Altintas, L. Wang, S. Shendre, M. Sharma, H. Sun, E. Mutlugun, H. V. Demir, *Adv. Mater.* **2020**, *32*, 1905824.
- [19] M. D. Tessier, P. Spinicelli, D. Dupont, G. Patriarche, S. Ithurria, B. Dubertret, *Nano Lett.* **2014**, *14*, 207.
- [20] Y. Kelestemur, B. Guzelturk, O. Erdem, M. Olutas, K. Gungor, H. V. Demir, *Adv. Funct. Mater.* **2016**, *26*, 3570.
- [21] J. Leemans, S. Singh, C. Li, S. Ten Brinck, S. Bals, I. Infante, I. Moreels, Z. Hens, *J. Phys. Chem. Lett.* **2020**, *11*, 3339.
- [22] F. Fan, P. Kanjanaboos, M. Saravanapavanantham, E. Beauregard, G. Ingram, E. Yassitepe, M. M. Adachi, O. Voznyy, A. K. Johnston, G. Walters, G.-H. Kim, Z.-H. Lu, E. H. Sargent, *Nano Lett.* **2015**, *15*, 4611.
- [23] Y. Kelestemur, B. Guzelturk, O. Erdem, M. Olutas, T. Erdem, C. F. Usanmaz, K. Gungor, H. V. Demir, *J. Phys. Chem. C* **2017**, *121*, 4650.
- [24] Y. Kelestemur, D. Dede, K. Gungor, C. F. Usanmaz, O. Erdem, H. V. Demir, *Chem. Mater.* **2017**, *29*, 4857.
- [25] G. H. V. Bertrand, A. Polovitsyn, S. Christodoulou, A. H. Khan, I. Moreels, *Chem. Commun.* **2016**, *52*, 11975.
- [26] A. Polovitsyn, Z. Dang, J. L. Movilla, B. Martín-García, A. H. Khan, G. H. V. Bertrand, R. Brescia, I. Moreels, *Chem. Mater.* **2017**, *29*, 5671.
- [27] C. Meerbach, R. Tietze, S. Voigt, V. Sayevich, V. M. Dzhegagan, S. C. Erwin, Z. Dang, O. Selyshchev, K. Schneider, D. R. T. Zahn, V. Lesnyak, A. Eychmüller, *Adv. Opt. Mater.* **2019**, *7*, 1801478.
- [28] A. A. Rossinelli, H. Rojo, A. S. Mule, M. Aellen, A. Cocina, E. De Leo, R. Schäublin, D. J. Norris, *Chem. Mater.* **2019**, *31*, 9567.
- [29] Y. Gao, X. Peng, *J. Am. Chem. Soc.* **2015**, *137*, 4230.
- [30] F. T. Rabouw, J. C. van der Bok, P. Spinicelli, B. Mahler, M. Nasilowski, S. Pedetti, B. Dubertret, D. Vanmaekelbergh, *Nano Lett.* **2016**, *16*, 2047.
- [31] S. Singh, R. Tomar, S. Ten Brinck, J. De Roo, P. Geiregat, J. C. Martins, I. Infante, Z. Hens, *J. Am. Chem. Soc.* **2018**, *140*, 13292.
- [32] I. Moreels, A. Di Giacomo, C. Rodà, A. H. Khan, *Chem. Mater.* **2020**, *32*, 9260.
- [33] Y. Chen, D. Chen, Z. Li, X. Peng, *J. Am. Chem. Soc.* **2017**, *139*, 10009.
- [34] C. Pu, X. Peng, *J. Am. Chem. Soc.* **2016**, *138*, 8134.
- [35] S. Ithurria, G. Bousquet, B. Dubertret, *J. Am. Chem. Soc.* **2011**, *133*, 3070.
- [36] A. Riedinger, F. D. Ott, A. Mule, S. Mazzotti, P. N. Knüsel, S. J. P. Kress, F. Prins, S. C. Erwin, D. J. Norris, *Nat. Mater.* **2017**, *16*, 743.
- [37] D. Chen, Y. Gao, Y. Chen, Y. Ren, X. Peng, *Nano Lett.* **2015**, *15*, 4477.
- [38] J. Li, L. Wang, J. Li, L. Wang, *Appl. Phys. Lett.* **2004**, *84*, 3648.
- [39] A. Hassinen, I. Moreels, K. De Nolf, P. F. Smet, J. C. Martins, Z. Hens, *J. Am. Chem. Soc.* **2012**, *134*, 20705.
- [40] Y. Yang, J. Li, L. Lin, X. Peng, *Nano Res.* **2015**, *8*, 3353.